Eco. Env. & Cons. 29 (January Suppl. Issue) : 2023; pp. (S484-S493)
Copyright@ EM International
ISSN 0971–765X

DOI No.: http://doi.org/10.53550/EEC.2023.v29i01s.074

Fe (II) Ions' Adsorption Kinetics and Thermodynamics on *Lagenaria siceraria* Stem Nano Carbon

A. Mangayarkarasi[1], S Arivoli[2*] and K. Veeravelan[3]

[1]PG and Research Department of Chemistry, Thiru Vi Ka Government Arts College (Affiliated to Bharathidasan University 620 024), Thiruvarur 610003, Tamilnadu, India.
[2,3*]PG and Research Department of Chemistry, Poompuhar College(AU) (Affiliated to Bharathidasan University 620 024), Melaiyur 609107, Tamilnadu, India

(Received 3 September, 2022; Accepted 9 November, 2022)

ABSTRACT

As severe a threat to the environment as global warming is heavy metal contamination. Nano carbon from *Lagenaria siceraria* Stem fiber has been used to examine the removal of Fe(II) ions from aqueous solution. It employs batch adsorption methods. We looked into the effects of contact time, initial adsorbent concentration, dose, and solution pH. The equilibrium adsorption data were connected with the Langmuir, Freundlich, Dubinin-Radushkevich, and Redlich-Peterson isotherm models. The adsorption procedure was advantageous, according to the isotherm analyses of RL values. The evaluation of thermodynamic parameters ΔH^0, ΔS^0, and ΔG^0. The data show that the adsorption was endothermic in nature and spontaneous. Pseudo-second-order, Elovich model, and intra-particle diffusion models were used to investigate the kinetics of adsorption. A pseudo-second-order adsorption reaction is suggested by kinetic investigations. This work demonstrates that intra-particles were crucial to the mechanism governing the adsorption of Fe(II) ions. For the removal of Fe(II) ions from aqueous solution, the Activated *Lagenaria siceraria* Stem Nano Carbon has a high adsorption capacity and adsorption rate.

Key words : *Adsorption, Fe(II) ions, kinetics, Activated Lagenaria Siceraria Stem Nano Carbon (ALSNC), Thermodynamic parameters.*

Introduction

Nowadays, one of the major concerns is environmental pollution. People's health is being adversely impacted by the environment's destruction and damage, which are caused by the population's sharp expansion and the accelerated development of industry. Different pollutants are released into wastewater, including organics, bacteria, viruses, heavy metal ions, and others. For ecological, evolutionary, nutritional, and environmental reasons, heavy metal ions are significant environmental contaminants because they are non-degradable and persistent. Industries that release Fe(II) into the environment include those that produce fertiliser, petrochemicals, electroplate, tan, process metals, and mine (Amin, 2008 and 2009; Gad and El-Sayed, 2009, Ganesh *et al.,* 2005. Garg; *et al.,* 2004. Worldwide, activated carbon has been utilised as an adsorbent in wastewater treatment applications, but due to its high cost and low efficiency, it is no longer an attractive option for usage in large quantities in small-scale companies. Research interest in creating adsorbents to replace pricey activated carbon has risen tremendously (Giri *et al.,* 2012). Lagenaria Siceraria Stem was used as an adsorbent in several studies on wastewater treatment because it is readily available, economically viable, and biodegradable

(Hameed *et al.,* 2007). Jordanian Pottery was also selected as an adsorbent because of its low cost, granular structure, insolubility in water, chemical stability, and local availability (Pavan *et al*., 2008).

Materials and Methods

Adsorption, mg/L: The *Lagenaria siceraria* stem collected from nearby Nagapattinam district was carbonized with Con. H_2SO_4 and activated around 1100 ^oC in a muffle furnace for 5 hrs. Then it was taken out, ground well to fine powder and stored in a vacuum desiccators.

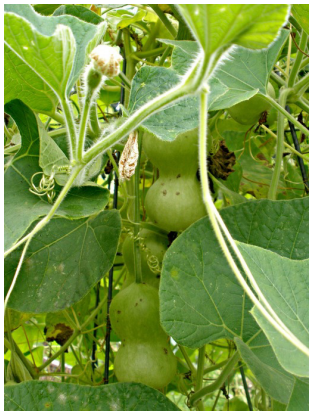

Lagenaria Siceraria Stem

Batch adsorption studies

The eradication of Fe(II) from activated *Lagenaria siceraria* stem nano-carbon was examined in relation to the consequences of numerous parameters. All of the chemicals utilised were of the highest purity AR grade that was easily obtainable in commerce. Ammonium Ferrous Sulphate Deca Hydrate was dissolved in the calculated amount of de-ionized water to create an adsorbate stock solution with 8.636 mg/L of Fe(II). The initial concentration of the stock solution (which ranged from 25 to 125 mg/L) was diluted to the necessary level. Each adsorption experiment used a 250 ml stopper glass flask containing 50 ml of known-concentration Fe(II) ion solution and 25 mg of activated *Lagenaria siceraria* Stem Nano Carbon. The mixture was agitated on a mechanical shaker for 60 minutes.

At the proper intervals, samples were taken out, and the adsorbent was separated by centrifugation at 1000 rpm for 10 minutes. An atomic absorption spectrophotometer was used to quantify the supernatant's residual Fe(II) concentration both before and after the treatment (Perkin Elmer, 2380). Fe(II) concentration of 50 mg/l for continuous Activated Lagenaria Siceraria Stem Nano Carbon was used to study the impact of pH on the rate of adsorption. With 0.1N HCl and 0.1N NaOH solution, the pH levels were adjusted. Different temperatures were used for the adsorption process (30^{o}C, 40^{o}C, 50 ^{o}C and 60 ^{o}C). This made it easier to calculate the effects of changes in thermodynamic parameters brought on by the temperature effect. The formula below can be used to calculate the quantity of adsorption at time t, qt(mg/g);

$$q_t = (C_0\text{-}C_t)V/\ W \ldots\ldots\ldots\ldots\ldots\ldots\ldots(1)$$

Where, V is the volume of solution (L), W is the mass of the adsorbent (g), and Ct is the concentration of Fe(II) ions in the liquid phase (mg/l) at any moment. The quantity of adsorption at equilibrium, qe(mg/g), was calculated using the following equation.

$$q_e = (\ C_0 - C_e)\ V/(W) \ldots\ldots\ldots\ldots\ldots\ldots..(2)$$

Where, C_0 and C_e are the liquid phase concentration of Fe(II) ions (mg/L) initially and at equilibrium. The removal percentage of Fe (II) ions can be calculated as:

$$\text{Removal \% of Fe (II)} = (C_0\text{-}C_e)/\ C_0 \times 100 \ldots. (3)$$

Where, C_0 is the initial concentration of the Fe(II) ions in solution (mg/l), and Ce is the equilibrium concentration of Fe(II) ions in solution(mg/l).

Results and Discussion

Effect of contact time on Fe(II) ions adsorption

One of the important parameters in the batch adsorption process is contact time. The procedure that was produced kept all of the parameters constant, with the exception of contact duration, temperature (30, 40, 50, and 60 °C), adsorption dose, and agitation speed (120 rpm). Figure 1 illustrates the highest removal of Fe(II) by Activated Lagenaria Siceraria Stem Nano Carbon, which needed contact time of 60 minutes. It was shown that removal of Fe(II) increased with contact time, and the best removal efficiency was attained in 30 minutes. The highest amount of adsorption takes place after 30 minutes, at which point the adsorption phase approaches equilibrium. This is the point at which the most Fe(II) can be absorbed under the given circum-

stances. Figure 1 depicts a single, smooth, continuous time variation curve and the creation of a monolayer covering the adsorbent's outer contact (Rahman *et al.* 2012).

Effect of Initial Fe(II) Concentration

To investigate the impact of initial Fe(II) ions on the amount of adsorption by increasing concentrations (25, 50, 75, 100, and 125 mg/L) under the same conditions of constant temperature (30, 40, 50, and 60 °C), pH 6.5, agitation speed (120 rpm), and 0.025 g of adsorbent dosage. The experimental results were reported, which illustrates the removal efficiency as a function of the starting concentration of Fe(II) ions. It demonstrates that as the initial Fe(II) concentration increases, the removal efficiency of Fe(II) decreases (II). Low Fe(II) ion concentrations result in a significant initial mole ratio compared to the accessible surface area of the adsorbent, which makes fractional adsorption independent of starting concentration. The proportion of Fe(II) ions, however, is dependent on the initial concentration of Fe(II) ions since there are fewer accessible sites for adsorption at higher concentrations.

Effect of adsorbent dosage

The impact of various adsorbent doses was examined using (25, 50, 100, 200 and 250 mg). 50 ml of a solution containing Fe(II) ions was used to stir them. The adsorbent dosages that affect the adsorption of Fe(II) ions by ALSNC are shown in Figure 2. It is clear that higher adsorbent doses will result in greater removal of Fe(II) ions. This happens as a result of an increase in the contact surface areas of the adsorbent. The likelihood of Fe(II) ions being adsorbed on adsorption sites would increase, as would the adsorption efficiency. Therefore, adsorbent dosage of 25 mg in 50 ml of adsorbate solution is used throughout all of the studies.

Effect of solution pH

The response One of the most critical aspects that affects how Fe(II) ions are adsorb to the sorbent material is pH. The chemical form of the heavy Fe(II) ion in the solution at a precise pH is accountable for the adsorption capacity (i.e. Pure ionic metal form or metal hydroxyl form). Additionally, the impact of adsorption might vary greatly due to various functional groups on the adsorbent surface that turn into active sites for the Fe(II) binding at a particular pH. Therefore, depending on the type of adsorbent, different optimum pH values will arise from an increase in pH, which may result in an increase or decrease in the adsorption. By injecting acid and base to the stock solution, the solution pH was changed from 3.0 to 9.0 to study the impact of pH on the percentage removal of Fe(II) ions. This rise may be caused by the existence of a negative charge on the adsorbent's surface, which may be responsive to the binding of Fe(II). The hydrogen ions compete with the Fe(II) ions for adsorption sites in the adsorbent when the pH is dropped. Additionally, the overall surface charge of the particles becomes positive, which prevents the binding of positively charged Fe(II) ions. On the other hand, a decrease in adsorption under a pH of >6.5 may be brought on by OH- ions occupying the adsorption sites, delaying their further approach to the adsorbent surface. The optimal pH range for the adsorption of the Fe(II) ions is 3.0 to 6.5, as illustrated in Figure 3, according to the experimental data.

Adsorption Isotherms

The interaction between the proportion or concentration of adsorbate that accumulates on the adsorbent and the equilibrium concentration of the dissolved adsorbate is described by an adsorption isotherm (Yuchen Tian, *et al.* 2022). A series of beakers holding 50 mL of Fe(II) ion solutions with an initial concentration of 25 mg/L were shaken vigorously at 30 °C to conduct equilibrium studies. The beakers also contained 0.025g of activated nano carbon. Agitation was present for one hour, which is more than enough time for equilibrium to be reached.

Freundlich adsorption isotherm

Based on equilibrium sorption on heterogeneous surfaces, the Freundlich adsorption isotherm was developed. This isotherm is derived on the grounds that the distribution of adsorption sites with respect to adsorption heat is exponential. The following equation represents the adsorption isotherm.

$$q_e = K_F C_e^{1/nF} \quad \ldots\ldots\ldots\ldots\ldots\ldots\ldots (4)$$

Which, can be linearized as

$$\ln q_e = \ln K_F + \frac{1}{n_F} \ln C_e \quad \ldots\ldots\ldots\ldots\ldots\ldots (5)$$

Where, q_e is the amount of Fe(II) adsorbed at equilibrium (mg/g) and C_e is the concentration of Fe(II) in the aqueous phase at equilibrium (ppm). K_F

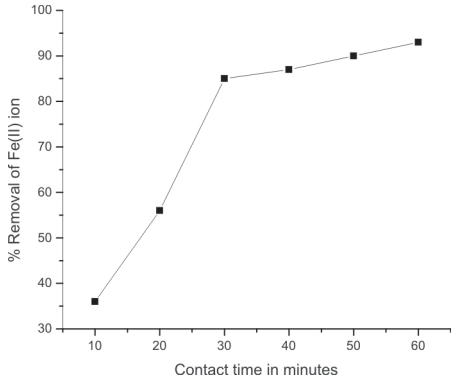

Fig. 1. Effect of Contact Time on the Removal of Fe(II) ion. [Fe(II)]=50mg/l; Temperature 30 ^{0}C; Adsorbent dose=0.025g/50ml.

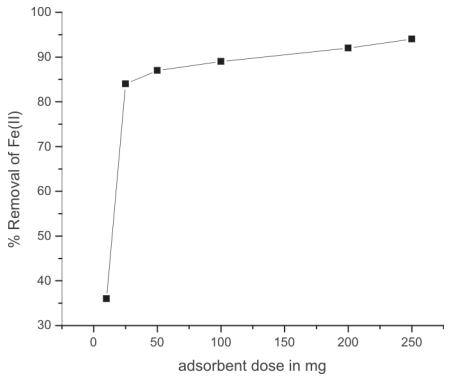

Fig. 2. Effect of Adsorbent dose on the Removal Fe(II) ion [Fe(II)]=50mg/l; Temperature 30 ^{0}C; Contact Time 60 min.

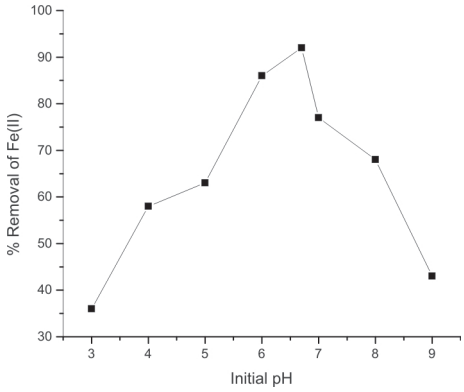

Fig. 3. Effect of Initial pH on the Removal of Fe(II) ion. [Fe(II)]=50mg/l; Temperature 30 ^{0}C; Adsorbent dose=0.025g/50 ml.

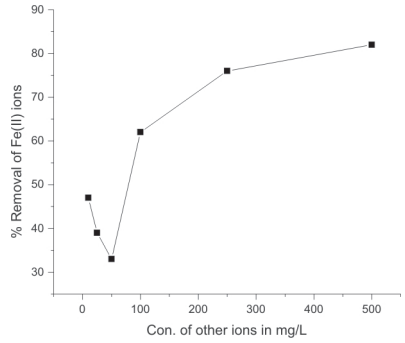

Fig. 4. Effect of Concentration of other ions on the Removal of Fe(II) ion [Fe(II)]=50 mg/l; Contact Time 60 min.; Adsorbent dose=0.025g/50 ml.

(L/g) and $1/n_F$ are the Freundlich constants related to adsorption capacity and sorption intensity, respectively.

The slope and intercept of the lnqe Vs ln Ce plot were used to determine the Freundlich constants KF and 1/nF. Table 1 displays the model's parameters. The size of KF demonstrated that ALSNC has a significant ability to adsorb Fe(II) from the aqueous solutions under evaluation. To be deemed a favourable adsorption, the Freundlich exponent, nF, must have values between 1 and 10 (i.e., 1/nF 1). It was shown that Fe(II) is positively adsorbed by ALSNC when the 1/nF value was smaller than 1. According to SSE and Chi-square statistics, the Freundlich isotherm did not provide a good fit to the experimental data.

Langmuir adsorption isotherm

According to the Langmuir adsorption isotherm, all sorption sites have an equal affinity for the adsorbate. In a linear form, the Langmuir isotherm (Patrolecco *et al.*, 2015) can be depicted as:

$$\frac{C_e}{q_e} = \frac{1}{q_m K_L} + \frac{C_e}{q_m} \quad .. (6)$$

Where q_e is the amount of Fe(II) adsorbed at equilibrium (mg/g), C_e is the concentration of Fe(II) in the aqueous phase at equilibrium (ppm), q_m is the maximum Fe(II) uptake (mg/g), and K_L is the Langmuir constant related to adsorption capacity and the energy of adsorption (g/mg).

To calculate the values of qm and KL, a linear plot of Ce/qe Vs Ce was used, and the resulting data were also shown in Table 1. The experiments were unable to reach the maximum value that the model projected. With an increase in temperature, KL's value fell. A strong adsorption affinity is indicated by a high KL value. The equilibrium param-

Table 1. Isotherms Parameter For The Adsorption Of Fe(ii) Ion Onto Alsnc

Model	Constant	Temperature (°C)			
		30	40	50	60
Freundlich	K_f (mg/g) (L/mg)$^{1/n}$	13.21	17.87	21.5	22.94
	n_F	1.778	2.155	2.464	2.463
Langmuir	Q_m (mg/g)	89.48	80.63	77.04	78.09
	K_L (L/mg)	0.13	0.212	0.297	0.345
Radlich-Peterson	g	0.438	0.536	0.594	0.594
	K_R (L/g)	0.076	0.056	0.047	0.044
Dubinin-Radushkevich	q_s (mg/g)	53.4	51.74	51.85	54.25
	$K_D \times 10^{-4}$ mol^2 kJ^{-2}	1.446	1.429	1.422	1.431

eter (RL), which is described in the following equation, was used by Weber and Chakraborti to express the Langmuir isotherm.

$$R_L = \frac{1}{1+K_L C_0} \quad .. (7)$$

Where, C_0 is the initial Fe(II) concentration (ppm). Four scenarios can be distinguished:

The sorption isotherm is unfavourable when RL exceeds 1, linear when RL is the same as 1, favourable when RL is in the range of 0 to 1, and irreversible when RL is zero. The values of the dimensionless separation factor (RL) for Fe(II) removal were calculated at various concentrations and temperatures. Table 1 shows that all concentrations and temperatures tested had values of RL for Fe(II) adsorptions on the ALSNC that were less than 1 and more than zero, indicating good adsorption.

The Langmuir isotherm offered a better fit to the adsorption data than the Freundlich isotherm did. The homogeneous distribution of active sites on the ALSNC surface may be the reason why the Langmuir isotherm matches the actual results so well because the Langmuir equation assumes that the adsorbent surface is energetically homogenous.

Redlich-Peterson adsorption isotherm

The properties of the Langmuir and Freundlich isotherms are incorporated into a single equation by the Redlich-Peterson(Hammed, 2009) adsorption isotherm, which has three parameters. The following is a description of the general isotherm equation:

$$q_e = \frac{K_R C_e}{1+a_R C_e^g} \quad .. (8)$$

The linear form of the isotherm can be expressed as follows:

$$\ln \frac{C_e}{q_e} = g \ln C_e - \ln K_R \quad .. (9)$$

Where, K_R (L/g) and a_R (L/mg) are the Radlich-Peterson isotherm constants and g is the exponent between 0 and 1. There are two limiting cases: Langmuir form for g = 1 and Henry's law for g = 0.

The isotherm constants g and KR can be calculated from the slope and intercept of a plot of ln Ce/qe Vs ln Ce. The KR values in Table 1 show that the adsorption capacity of the ALSNC reduced as the temperature goes up. A favourable adsorption is also indicated by the fact that the value of g is between 0 and 1.

Dubinin-Radushkevich adsorption isotherm

Another isotherm equation is the Dubinin-Radushkevich adsorption isotherm (Gupta *et al.*, 1988). It is presumable that the sorption curve's characteristic has something to do with the adsorbent's porosity. The isotherm's linear form is represented as follows:

$$\ln q_e = \ln Q_D - B_D \left[RT \ln\left(1+\frac{1}{C_e}\right)\right]^2 \quad .. (10)$$

Where BD is the Dubinin-Radushkevich constant (mol^2/kJ^2) and QD is the maximum sorption capacity (mol/g). The isotherm constants BD and QD can be found by plotting lnqe vs RTln(1+1/Ce) and analysing the slope and intercept.

Kinetic parameters

$$k_1,\ k_2,\ (q_e-q_t),\ k_1,\ (q_e-q_t)$$

Based on kinetic studies, the rate and mechanism of the adsorption process can be clarified. There are two separate mechanisms that could account for Fe(II) adsorption on solid surfaces: Fe(II) molecules initially attach quickly to the adsorbent surface, fol-

lowed by rather slow intra-particle diffusion. The pseudo-first-order, pseudo-second-order, and intra-particle diffusion models were used to examine the adsorption kinetics of the Fe(II) (Khan and Singh, 1987). The equations for each of these models' linear modes are shown below quation No. 11 and 12.

Where qe and qt stand for the amount of Fe(II) adsorbed (mg/g) at equilibrium and at any time, t (min), respectively, and k^1 and k^2 are the equilibrium rate constants of the pseudo-first order and pseudo-second order models, respectively.

A straight forward kinetic model called the pseudo-first order model, developed by Lagergren in 1898, is used to calculate the rate of the surface adsorption reaction. There was a linear correlation between the values of ln (q^e - q^t) and t. The values of k1 were calculated from the slope of the plot by ln (q_e - q_t) Vs t, which should show a linear connection. The first-order equation of Lagergren is typically appropriate for the initial stage of the adsorption processes, but it does not always fit well with the complete range of contact time.

In the pseudo-second order model, the second-order rate constant, k_2, was calculated using the slope and intercept of the t/q_t Vs t plot. The results of Karagoz *et al.* and Hameed *et al.* are in agreement with assertion that Fe(II) adsorption followed the pseudo-second order model, where the R^2 value was 0.999. But neither the pseudo-first order nor the pseudo-second order kinetic models can explain the mechanism of Fe(II) diffusion into the adsorbent pores

Simple Elovich Model

The simple Elovich model is expressed in the form,

$q_t = \alpha + \beta \ln t$, mg/L ……..(13)

Where qt is the quantity that has been adsorbed at time t, and and are constants discovered by experimentation. The simple Elovich kinetic should be applicable if qt Vs lnt is plotted as a linear relationship. The Elovich kinetics of Fe(II) on ALSNC at different starting concentrations (10, 20, 30, 40, and 50 mg/l), volume 50 ml (each), adsorbent dosage 0.025g, temperature 30 °C, and pH 6.5.

The intra-particle diffusion model

According to Weber and Morris (Al Duri *et al.*, 1990), the following kinetic model can be used to determine whether or not an intra-particle diffusion model is responsible for the adsorption process. Typically, it is stated as

$q_t = K_{id}\, t^{1/2} + C$……..(15)

Where K_{id} (in mg/g/$min^{1/2}$) is the intra-particle rate constant, c is the intercept, and qt (in mg/g) is the amount of Fe(II) ions adsorbed at time t. The intra-particle rate constant can be calculated from the slope of the qt Vs $t^{1/2}$. The value of C provides information on the thickness of the boundary layer. The values show that the sorption rate is controlled by

Kinetic Models and Their Linear Forms .... 11 & 12

Model	Nonlinear Form	Linear Form	Number of Equation
Pseudo-first-order	$dq_t/d_t = k_1(q_e-q_t)$	$\ln (q_e-q_t) = \ln q_e - k_1 t$	-11
Pseudo-second-order	$dq_t/d_t = k_2(q_e-q_t)^2$	$t/q_t = 1/k^2q_e^2 + (1/q_e)t$	-12

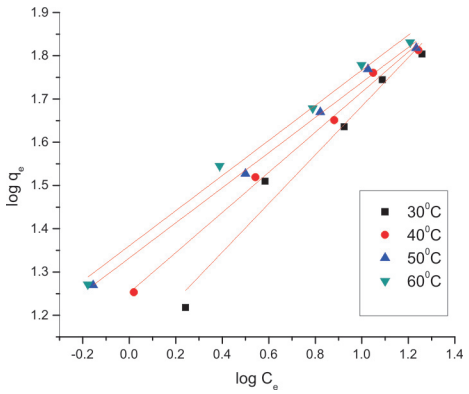

Fig. 5. Equilibrium parameters for the Adsorption of Fe(II) Ion onto ALSNC

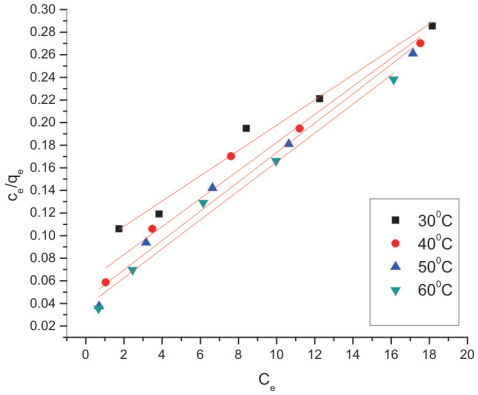

Fig. 6. The Kinetic Parameters for the Adsorption of Fe(II) Ion onto ALSNC

the intra-particle diffusion process.

Thermodynamic parameters

K_0, Equ. No : (16), $\Delta G^0 = \Delta H^0 - T\Delta S^0$ .. (16)

Equilibrium constant (K_0) change with temperature was used to calculate thermodynamic parameters (Chien and Clayton, 1980) such as standard free energy (ΔG^0), standard enthalpy change (ΔH^0), and standard entropy changes (ΔS^0). The following equation can be used to calculate the change in free energy.

$\Delta G^0 = -RT \ln K^o$…….. (15)

Where ΔG^0 is the change in sorption's free energy (measured in kJ/mol), K^o is the equilibrium constant, T is the temperature (measured in K), and R is the constant of universal gas. As a function of temperature, the enthalpy change of sorption can be used to express the free energy change as follows.

$\Delta G^0 = \Delta H - T\Delta S$…… (15)

The adsorption coefficient K_0 can be obtained by combined and rearranging Eqs (15) and (16)

$\ln K_0 = \Delta H^0 / RT + \Delta S^0/R$……..(17)

Where ΔS^0 is the entropy change of sorption (KJ/mol) and ΔH^0 is the standard heat changes of the sorption. The slope and intercept of the linear plot of the standard enthalpy and entropy changes are calculated versus 1/T. The values for the thermodynamic parameters are reported in equation (16) and come from the equation (17) for the sorption of Fe(II) ions on activated *Lagenaria siceraria* stem nano carbon. The exothermic nature of the sorption process for Fe(II) on activated Lagenaria siceraria stem nanocarbon is confirmed by the negative values of free energy changes and the negative values of ΔH^0. The positive ΔS^0 values during the sorption of Fe(II) ions on the Activated *Lagenaria Siceraria* Stem Nano Carbon demonstrate increased unpredictability at the solid-solution interface.

The values of activation energy (Ea) and sticking probability (S*) were computed from the experimental data to support that physical adsorption is the major process. They were determined using the following modified Arrhenius type surface coverage (θ) equation:

$$\theta = \left(1 - \frac{C_e}{C_i}\right) \text{……. (18)}$$

$$S^* = (1-\theta)_e \frac{-E_a}{RT} \text{…… (19)}$$

The sticking probability, S*, is a function of the adsorbate/adsorbent system under consideration but must satisfy the condition $0 < S^* < 1$ and is dependent on the temperature of the system. The values of Ea and S* can be calculated from slope and intercept of the plot of ln(1-θ) versus 1/T respectively (As shown in Fig. 5).

The reaction is spontaneous in nature as ΔG^0 values are negative at all the temperature studied. Again positive ΔH^0 value confirms that the sorption is endothermic in nature. The positive value of ΔS^0 reflects the affinities of the adsorbents for the Fe(II). The result as shown in Fig. 5 indicate that the probability of the Fe(II) to stick on surface of biomass is very high as $S^* << 1$, these values confirm that, the sorption process is physisorption (Weber and Morris, 1964).

FT-IR Study

Thermo Scientific, (USA) FT-IR (NICOLET iS50) spectra of ALSNC samples are shown in the images both before and after adsorptions. Figure 7, respectively a and b. The spectra show that there are surface groups on the surface of the adsorbent. Between them, the peak intensities differ substantially. The intensity of almost all of the absorptions bands clearly varies between the carbons, which is an indication of how differently dense the various functional groups are. Following adsorption, some peaks disappear because of desorption into the adsorbate, while electrostatic forces cause a few others to have their wave numbers slightly shift upward or downward. There are no new peaks now that adsorption has established that no new chemicals are being produced. As can be seen in the figures, the adsorption frequencies are almost equal, and it is thought that they had minimal effect on the functional groups, supporting the notion that only physisorption had taken place. Following adsorption, some peaks disappear because of desorption into the adsorbate, while electrostatic forces cause a few others to have their wave numbers slightly shift upward or downward. As can be seen in the figures, the adsorption frequencies are almost equal, and it is thought that they had minimal effect on the functional groups, supporting the notion that only physisorption had taken place.

XRD Study

The X-ray Diffraction Research was carried out using the Rigaku Corporation, Japan X-ray Diffractometer 40KV / 30mA, Model XRD 6000 SHIMADZU. The diffraction patterns of the adsorbent ALSNC before and after *Lagenaria siceraria* adsorption are shown in Figures 8 (a) and (b). The graphs unmistakably demonstrate that the adsorbent's spectra before and after adsorption are identical. This may be so because adsorption modifies the chemical makeup of the adsorbent's surface only slightly, if at all. Physically, the adsorption is controlled by weak Van der Waals forces.

SEM

The SEM micrographs in Figures 9 (a) and (b) show the ALSNC-derived ALSNC's uneven surface and significant porosity. Large macropores present in these carbonaceous materials frequently allow adsorbates to pass through and enter the microporous system. Before and after adsorption, the surface morphology of ALSNC was examined using scanning electron microscopy (SEM). The matching SEM micrographs are displayed in figures 9 (a) and (b) utilising a JEOL JSM 6390 at a 20kV accelerating voltage. At such magnification, the ALSNC particles showed rough areas of surface with clearly visible

Figures 7 (a,b) FT-IR spectrum of *ALSNC*

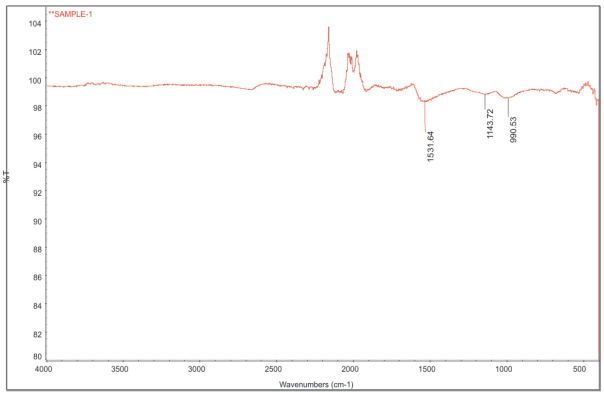

Fig. 7(a). Before adsorption

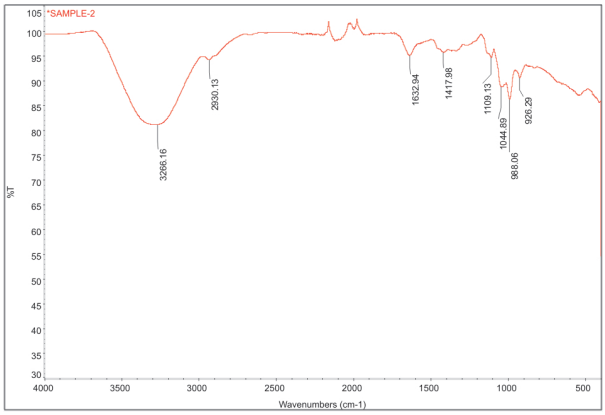

Fig. 7(b). After adsorption

Figures 8 (a,b) XRD Patern *ALSNC*

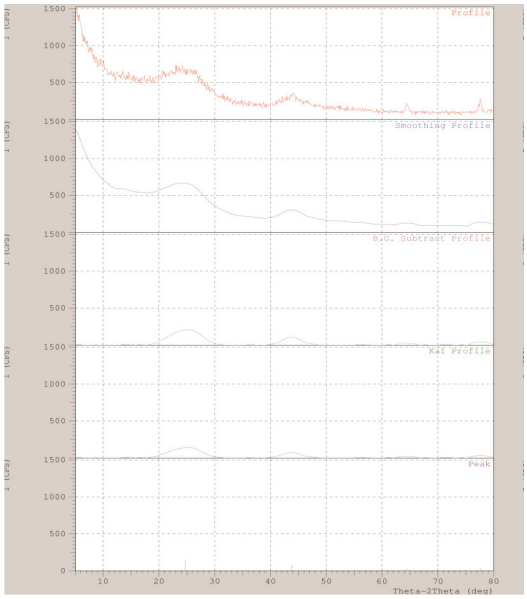

Fig. 8 (a) Before adsorption

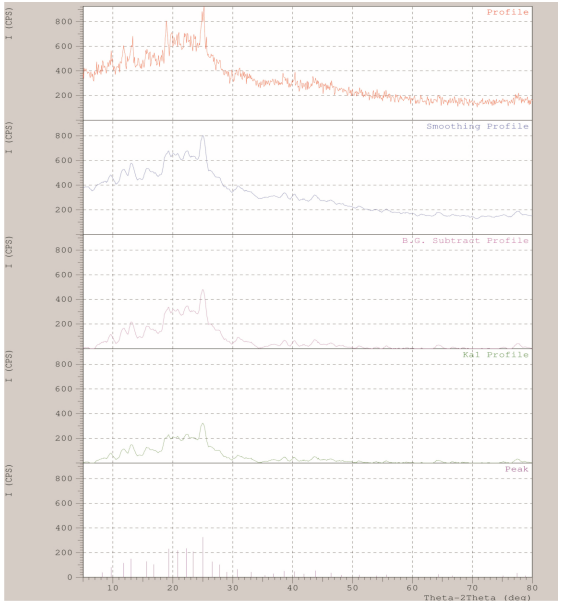

Fig. 8 (b) After adsorption

Figs 9 (a,b) SEM micrograph of *ALSNC*

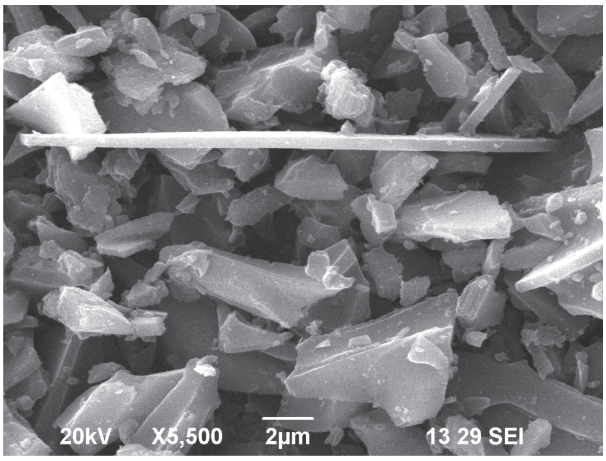

Fig. 9(a). Before adsorption

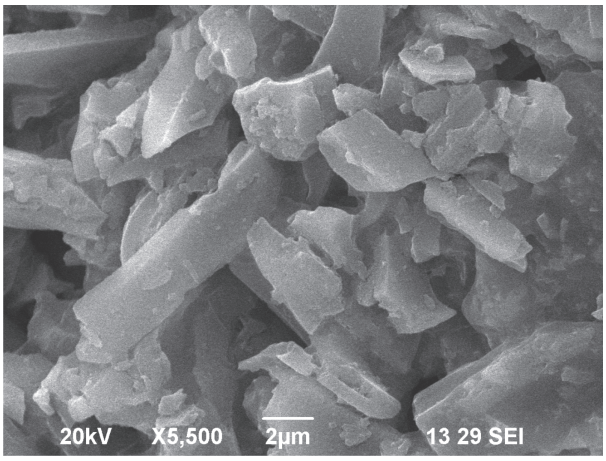

Fig. 9(b). After adsorption

micropores. This metallic element was not distributed uniformly across the surface of the carbon because the majority of the minerals in biomass are not lost during the pyrolysis procedure and stay on the ALSNC structure.

Conclusion

In this investigation, the Fe(II) adsorption on activated *Lagenaria siceraria* stem nano-carbon was investigated. From this study, were discovered. Because no chemical bonds are formed between the adsorbent and adsorbate, this adsorption has pseudo-second order kinetics and belongs to the category of physisorption. These researches are appropriate for the fruendlich and Langmuir isotherm model. The thermodynamic analysis finds negative ΔG^o, positive ΔH^o and ΔS^o values, which support the conclusion that this adsorption is physical, spontaneous, and possible in nature. According to isotherm and kinetic studies, the ALSNC can adequately adsorb Fe(II) ions. Fe(II) ion adsorption on ALSNC was demonstrated to be a spontaneous and physical process by thermodynamic analysis.

References

Amin, N.K. 2008. Removal of reactive dye from aqueous solutions by adsorption onto activated carbons prepared from sugarcane bagasse pith. *Desalination.* 223(1) : 152-161.

Amin, N.K. 2009. Removal of direct blue-106 dye from aqueous solution using new activated carbons developed from pomegranate peel: Adsorption equilibrium and kinetics. *Journal of Hazardous Materials.* 165(1-3): 52-62.

Al Duri, B., Mckay, G., El Geundi, M.S. and Wahab Abdul, M.Z. 1990. Three Resistance Transport Model for dye Adsorption onto Bagasse Pitch. *J. Environ. Eng. Div. ASCE.* 116:487.

Chien, S.H. and Clayton, W.R. 1980. Application of Elovich Equation to the kinetics of Phosphate release and sorption on soil. *Soil Sci. Sco, Am. J.* 44 265 – 268.

Gad, H.M. and El-Sayed, A.A. 2009. Activated carbon from agricultural by-products for the removal of Rhodamine-B from aqueous solution. *Journal of Hazardous Materials.* 168(2) :1070-1081.

Ganesh, P.S., Ramasamy, S., Gajalakshmi and Abbasi, S. 2005. Extraction of volatile fatty acids (VFAs) from water hyacinth using inexpensive contraptions and the use of the VFAs as feed supplement in conventional biogas digesters with concomitant final disposal of water hyacinth as vermicompost. *Biochemical Engineering Journal.* 27(1): 17-23.

Garg, V. M., Amita, R., Kumar and Gupta, R. 2004. Basic dye (methylene blue) removal from simulated wastewater by adsorption using Indian Rosewood sawdust: a timber industry waste. *Dyes and Pigments.* 63(3) : 243-250.

Giri A.K., Patel, R. and Mandal, S. 2012. Removal of Cr (VI) from aqueous solution by *Eichhornia crassipes* root biomass-derived activated carbon. *Chemical Engineering Journal.* 185: 71-81.

Gupta, G. S., Prasad, G. and Singh, V. N. 1988. Removal of Chrome Dye from Carpet Effluents using Coal II (Rate process). *Environ. Technol. Lett.* 9: 1413.

Hameed, B., Ahmad, A and Latiff, K. 2007. Adsorption of basic dye (methylene blue) onto activated carbon prepared from rattan sawdust. *Dyes and Pigments.* 75(1): 143-149.

Hammed, B.H. 2009. A novel agricultural waste adsorbent

for the removal of cationic dye fron aqueous solution. *Journal of hazardous materials.* 162: 305- 311.

Khan, A. A. and Singh, R. P. 1987. Adsorption thermodynamics of carbofuran on Sn (IV) arsenosilicate in H^+, Na^+ and Ca^{2+} forms. *Colloid & Surfaces.* (24) : 33- 42.

Pavan, F.A., Mazzocato, A.C. and Gushikem, Y. 2008. Removal of methylene blue dye from aqueous solutions by adsorption using yellow passion fruit peel as adsorbent. *Bioresource Technolog.* 99(8): 3162-3165.

Rahman, M.A., Amin, S.R. and Alam, A.S. 2012. *Removal of Methylene Blue from Waste Water Using Activated Carbon Prepared from Rice Husk. Dhaka University Journal of Science.* 60(2) : 185-189.

Patrolecco, L., Silvio Capri, S. and Ademollo, N. 2015. Occurrence of selected pharmaceuticals in the principal sewage treatment plants in Rome (Italy) and in the receiving surface waters. *Environ. Sci. Pollut. Res.* 22: 5864–5876.

Weber, T. W. and Chakravorti, R.K. 1974. *Pore and Solid diffusion models for fixed bed adsorbers. J. Am. Inst, Chem. Eng.* 20: 228.

Weber, W.J. and Morris, J.C. 1964. Kinetics of adsorption on Carbon from solution. *J. Sanitary Eng, Div.* 90 : 79.

Yuchen Tian,, Anggrek C., Nusantara, Thamir Hamoh, Aldona Mzyk, Xiaobo Tian, Felipe Perona Martinez, Runrun Li, Hjalmar P., Permentier and Romana Schirhagl, 2022. *Functionalized Fluorescent Nanodiamonds for Simultaneous Drug Delivery and Quantum Sensing in HeLa Cells.* 14 (34) : 39265-39273.